

# Determination of the Superfluid Gap in Atomic Fermi Gases by Quasiparticle Spectroscopy

André Schirotzek, Yong-il Shin, Christian H. Schunck and Wolfgang Ketterle

*Department of Physics, MIT-Harvard Center for Ultracold Atoms, and Research Laboratory of Electronics, Massachusetts Institute of Technology, Cambridge, Massachusetts, 02139*

(Dated: August 9, 2021)

We present majority and minority radiofrequency (RF) spectra of strongly interacting imbalanced Fermi gases of  ${}^6\text{Li}$ . We observed a smooth evolution in the nature of pairing correlations from pairing in the superfluid region to polaron binding in the highly polarized normal region. The imbalance induces quasiparticles in the superfluid region even at very low temperature. This leads to a local bimodal spectral response, which allows us to determine the superfluid gap  $\Delta$  and the Hartree energy  $U$ .

PACS numbers: 05.30.Fk 03.75.Ss 32.30.Bv 67.90.+z

Pairing and superfluidity in fermionic systems are intricately related phenomena. In BCS theory [1], describing conventional superconductors, the emergence of superfluidity is accompanied by the opening of a gap in the excitation spectrum of the superfluid. This gap can be interpreted as the minimum energy required to break a Cooper pair or, equivalently, to create an elementary excitation, a so-called quasiparticle, inside the superfluid.

However, strongly correlated systems show a more complicated behavior. There are gapless fermionic superfluid systems, as is the case for high temperature superconductors [2] or for superconductors with magnetic impurities [3]. On the other hand, there are numerous examples of systems with an excitation gap in the normal state, e.g. a high temperature superconductor above its superfluid transition temperature exhibiting a pseudogap [2] or a semiconductor.

Here, we use radiofrequency spectroscopy to investigate the nature of pairing and the relation between pairing and superfluidity in a strongly interacting system of ultracold atomic Fermions.

We can spectroscopically distinguish the superfluid and the polarized normal fluid by introducing excess fermions into the system. In a superfluid phase described by BCS theory, the excess particles can be accommodated only as thermally excited quasiparticles. A double-peaked spectrum reflects the co-existence of pairs and unpaired particles. In the normal phase, at large spin polarization, the limit of a single minority particle immersed into a Fermi sea is approached, which can be identified as a polaron [4, 5, 6, 7]. Here the system can be described in the framework of Fermi liquid theory and no stable pairs exist. We find that these different kinds of pairing correlations are smoothly connected across the critical density imbalance [8], also called the Clogston-Chandrasekhar limit of superfluidity [9, 10].

Excess fermions in a low-temperature superfluid constitute quasiparticles populating the minimum of the dispersion curve. The RF spectrum of a superfluid with such quasiparticles shows two peaks, which, in the BCS

limit, would be split by  $\Delta$ , the superfluid gap. Therefore, RF spectroscopy of quasiparticles is a direct way to observe the superfluid gap  $\Delta$  in close analogy with tunneling experiments in superconductors [11]. From the observed spectrum we can also determine a Hartree term [12], whose inclusion turned out to be crucial.

For this study, we have combined several recently developed experimental techniques: The realization of superfluidity with population imbalance [13] leading to phase separation [8, 13, 14], tomographic RF spectroscopy [15], in-situ phase contrast imaging with 3D reconstruction of the density distributions [8]. In order to minimize final state effects [16] we have prepared an imbalanced mixture of states  $|1\rangle$  and  $|3\rangle$  of  ${}^6\text{Li}$  (corresponding to  $|F = 1/2, m_F = 1/2\rangle$  and  $|F = 3/2, m_F = -3/2\rangle$  at low field) in an optical dipole trap at a magnetic field of  $B = 690$  G, at which there is a Feshbach scattering resonance between the states  $|1\rangle$  and  $|3\rangle$  [16, 17]. Evaporative cooling at  $B = 730$  G is performed by lowering the power of the trapping light. After equilibration an RF pulse was applied for  $200 \mu\text{s}$  selectively driving a hyperfine transition from state  $|1\rangle$  or  $|3\rangle$  to state  $(|2\rangle|F = 1/2, m_F = -1/2\rangle$  at low field). The RF power was kept constant for all experimental results presented. Immediately after the RF pulse an absorption image was taken of the atoms transferred into state  $|2\rangle$ .

The spectra were correlated to the local Fermi energy  $\epsilon_{F\uparrow} = \frac{\hbar^2}{2m} (6\pi n_{\uparrow})^{2/3}$  of the majority density  $n_{\uparrow}$  and to the local polarization  $\sigma_{loc} = \frac{n_{\uparrow} - n_{\downarrow}}{n_{\uparrow} + n_{\downarrow}}$  which is a measure of the local excess fermion population. As in a previous publication [8] the local densities were measured using phase contrast imaging and 3D reconstruction using the inverse Abel transformation.

The RF spectra shown in fig. 1 reveal a gradual change in the nature of the pairing correlations. The balanced superfluid is characterized by identical spectral responses of majority and minority particles and has been the subject of previous studies, see [18, 19, 20] and references therein. In the polarized superfluid region [8, 21] (and references therein) the minority spectrum perfectly

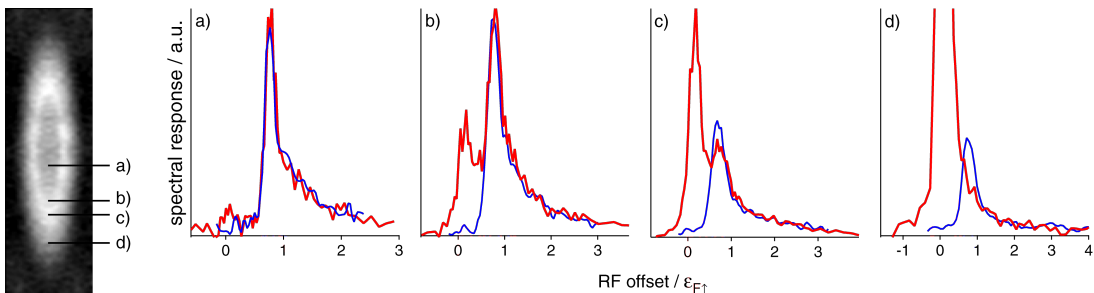


FIG. 1: (Color online) Tomographically reconstructed RF spectra for various regions of the atomic sample at unitarity. a) Balanced superfluid, b) polarized superfluid, c) moderately polarized transition region and d) highly polarized normal region. The panel on the left shows a phase contrast image of the atomic cloud before RF excitation. The positions of the spectra a) to d) are marked in the phase contrast image and by the arrows in figure 2 which displays all our results in the unitary limit. Red: Majority spectrum, blue: Minority spectrum. Local polarizations  $\sigma_{loc}$  and local temperature  $T/T_F$ , respectively: a)  $-0.04(2)$ ,  $0.05(1)$ , b)  $0.03(1)$ ,  $0.06(1)$ , c)  $0.19(1)$ ,  $0.06(2)$ , d)  $0.64(4)$ ,  $0.10(2)$ . The negative value in a) implies that the local polarization as inferred from phase-contrast imaging underestimates  $\sigma_{loc}$  by up to 0.05.

matches the pairing peak of the majority spectrum, locally coexisting with the quasiparticle spectral contribution, resulting in a local double peak structure of the majority spectrum (see fig. 1b). The spectrum suggests that the majority population can be divided into two distinct parts: One part consisting of pairs forming the superfluid, the other part consisting of quasiparticle excitations in the form of excess fermions. Therefore, a natural interpretation of the RF spectrum is to identify one peak as a Stokes process (RF creates a quasiparticle excitation) giving rise to the dissociation part of the RF spectrum and the other as an Anti-Stokes process (RF destroys a quasiparticle excitation).

As the local imbalance is further increased beyond the superfluid to normal (SF-N) transition [22], see fig. 1d, the majority spectrum no longer shows a local double-peak structure. This is consistent with theoretical work [23, 24] attributing the double peak structure in the normal phase in previously reported RF spectra [25, 26] to the inhomogeneous density distribution. For increasing spin polarization the majority and minority pairing peaks lose spectral overlap. We interpret the missing overlap as indication that the minority atoms are no longer bound in pairs, each of them interacting with more than one majority atom, a situation we refer to as polaronic binding. We have seen [22] that on the BEC side of the Feshbach resonance the overlap between minority and majority spectra does not depend strongly on the presence of excess fermions. This is expected in a molecular picture, where the pairing character is independent of the presence of excess fermions. At unitarity, within our experimental resolution, the overlap starts to decrease at the superfluid-to-normal interface, see fig. 1c. This raises the question whether at unitarity a local probe of the microscopic pairing, like RF spectroscopy, can distinguish whether the system is superfluid or not.

Even when the spectral overlap decreases, there is still

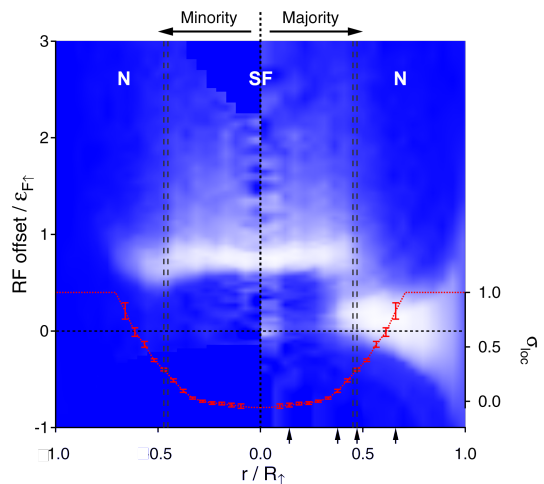


FIG. 2: (color online) Spatially resolved RF spectra of an imbalanced Fermi gas at unitarity. a) The right half shows the majority spectra as a function of position in the trap expressed in terms of the majority Fermi radius  $R_{\uparrow}$ , the left half displays the minority spectra. The superfluid to normal transition region is marked by the gray vertical lines. The local polarization  $\sigma_{loc}$  is given by the dashed red line. The error bars are the standard deviation of the mean value. The arrows indicate the position of the four spectra shown in fig. 1. The image is a bilinear interpolation of 2500 data points, each plotted data point in the image is the average of three measured data points. The spatial resolution of the image is  $0.045 \cdot R_{\uparrow}$ .

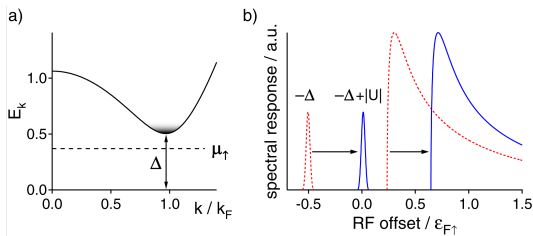


FIG. 3: (color online) Creation and spectroscopy of quasiparticles. a) Population imbalance thermally generates quasiparticles even at low temperatures comparable to  $\Delta - \mu_{\uparrow}$ .  $\mu_{\uparrow}$  is the chemical potential of the majority component. b) The RF spectrum consists of a quasiparticle peak at negative frequencies and the pair dissociation spectrum at positive frequencies (dotted line). On resonance, the Hartree contribution  $U$  acts as an effective attraction and hence shifts the entire spectrum into the positive direction.

equal response to the RF excitation in the high frequency tails, see fig. 1c and fig. 1d. These tails correspond to large momentum components in the interparticle wave function and hence address the short range physics. We expect this part of the spectrum to be insensitive to changes in the binding at large distances.

The direct comparison between majority and minority spectra clarifies our previous experimental results on minority RF excitation spectra in the  $|1\rangle - |2\rangle$  mixture [26], in which we concluded that there is strong pairing in the normal phase. However, the observed spectral gap in the normal phase should not be interpreted as a signature of pairing but rather as strong pairing correlations in the form of a polaron as suggested in [27, 28, 29]. The change in pairing correlations is indiscernible in the minority spectrum alone, but shows up in the spectral overlap with the majority spectrum.

We now turn to a quantitative analysis of the spectral peaks in the superfluid phase for small density imbalance, and to the determination of the superfluid gap. Earlier work [15, 25] tried to determine the gap from the onset of the pair dissociation spectrum. However, the RF spectrum is not only sensitive to final state interactions, it is also shifted by Hartree energies [12, 30], as we show here. Furthermore, RF spectroscopy can excite all fermions, even deep in the Fermi sea [18]. Therefore, the onset of the pair dissociation spectrum occurs for atoms with momentum  $k = 0$  and, in the BCS limit depends quadratically on the gap parameter ( $\omega_{th} = \frac{\Delta^2}{2\epsilon_F}$ ). The excitation gap can be directly observed if quasiparticles near the dispersion minimum are *selectively* excited, as in tunnelling experiments.

Our solution is to study not the ground state of a superfluid, but excited states where quasiparticles are present. In a simple BCS description, quasiparticles are in pure momentum states, but increase the total energy of the system because their momentum state is no longer

available to the other particles for pairing. Consequently, in an excitation spectrum, quasiparticles appear at negative frequencies relative to the bare atomic transition frequency. The lowest energy quasiparticle appears at frequency  $-\Delta$ , see fig. 3.

Final state interactions and Hartree terms can also create line shifts, and two peaks are needed for analysis, the dissociation peak and the quasiparticle peak in our case. In essence, it is the separation between the peaks in spectra like fig. 1b, which allows us to determine  $\Delta$ .

Thermal population of quasiparticles requires a temperature on the order of the excitation gap  $\Delta$ . At unitarity, this temperature can be estimated to be 95% of the critical temperature, away from the low temperature limit addressed in this letter. Indeed, in samples of equal population of the spin states we were not able to spectroscopically resolve any local double peak structures [22]. This problem can be overcome by introducing density imbalance between the constituents: The Fermi pressure (chemical potential  $\mu_{\uparrow}$ ) of majority atoms forces a finite quasiparticle occupation into the superfluid region already at very low temperature. This allows us to selectively populate quasiparticles at the minimum of the dispersion curve see fig. 3a.

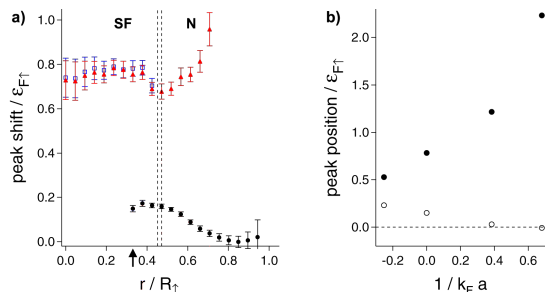


FIG. 4: (color online) a) Normalized peak positions of pairing peaks and quasiparticle peak at unitarity as a function of position in the trap. The SF-N boundary is marked by the dashed vertical lines. The arrow indicates the limit of low quasiparticle population relevant for b). Majority: blue open squares (pairing peak) and solid black circles (quasiparticle peak), Minority: solid red triangles. b) Pairing peak and quasiparticle peak positions as a function of the local interaction strength  $1/k_F a$  in the limit of small local imbalance (see arrow in a). Pairing peak: Solid circles, quasiparticles peaks: Open circles.

In figure 4a the position of the peaks of the majority and minority spectra are plotted normalized by  $\epsilon_{F\uparrow}$  as a function of position in the trap for the unitary limit [22]. The peak positions are proportional to the local Fermi energy inside the superfluid region within our experimental resolution. In the region of superfluidity with finite polarization the spectra show local double peaks. The position of the two peaks in the limit of small polarization is depicted in fig. 4b for various interaction strengths.

TABLE I: Superfluid gap  $\Delta$ , Hartree term  $U$  and final state interaction  $E_{final}$  in terms of the Fermi energy  $\epsilon_{F\uparrow}$  for various interaction strengths  $1/k_F a$ .

$1/k_F a$	$\Delta$	$U$	$E_{final}$
-0.25	0.22	-0.22	0.22
<b>0</b>	<b>0.44</b>	<b>-0.43</b>	<b>0.16</b>
0.38	0.7	-0.59	0.14
0.68	0.99	-0.87	0.12

It was unexpected that the quasiparticles appear at positive frequencies (relative to the atomic transition frequency). This is caused by the presence of Hartree terms [12], resulting in an overall shift of the systems energy and the RF spectrum [22]. In the weakly interacting limits, the Hartree term reduces to a simple mean field shift. In the strongly interacting regime one has to resort to QMC calculations [30, 31, 32] for a numerical value of  $U$ .

In a mean-field description of the balanced superfluid starting from the BCS-Leggett ansatz for the BEC-BCS crossover [18] taking into account the Hartree term  $U$ , the dispersion relation of the quasiparticles can be expressed as  $E_k = \sqrt{\Delta^2 + (\epsilon_k + U - \mu)^2}$  [12] where  $\epsilon_k = \frac{\hbar^2 k^2}{2m}$  is free particle kinetic energy and  $\mu$  is the chemical potential. This mean-field formalism gives the analytic expression for the two peak positions. A quasiparticle at the minimum of the dispersion curve will respond at an RF offset of  $\omega_{RF} = -E_{k_{min}} - \mu + \epsilon_{k_{min}} = -\Delta - U$ , and the maximum of the pair dissociation spectrum occurs at  $\hbar\omega_{max} = \frac{4}{3} \left( \sqrt{\mu'^2 + \frac{15}{16}\Delta^2} - \mu' \right) - U \simeq \frac{4}{3}\omega_{th} - U$ , where  $\mu' = \mu - U$  and  $\omega_{th}$  is the dissociation threshold (which is at momentum  $k = 0$ ).

We determined the superfluid gap  $\Delta$  and the Hartree energy  $U$  from the peak positions in the limit of small density imbalance ( $\sigma_{loc} \simeq 0.03$ ). At unitarity with the chemical potential  $\mu = 0.42 \epsilon_{F\uparrow}$ , confirmed in previous experiments, see [33] and references therein, we obtained  $\Delta = 0.44 \epsilon_{F\uparrow}$  and  $U = -0.43 \epsilon_{F\uparrow}$ , in excellent agreement with the predicted values  $\Delta_t = 0.45 \epsilon_{F\uparrow}$  and  $U_t = -0.43 \epsilon_{F\uparrow}$  from QMC calculations [34]. Our determined values for  $\Delta$  and  $U$  values suggest the minimum of the quasiparticle dispersion curve to occur at  $k_{min} \simeq 0.9k_F$ . Table I shows the gap and Hartree energy for various interaction strengths. Away from unitarity we relied on QMC calculations for the chemical potential  $\mu$  [35].

For an accurate quantitative comparison [22] final state interactions, also listed in table I, had to be taken into account. The effect of final state interactions is an overall mean field shift of  $E_{final} = \frac{4\pi\hbar^2 a}{m} n$ . This shift affects both the quasiparticle peak and the pairing peak equally.

In conclusion, we have performed spatially resolved RF spectroscopy of majority and minority components of a trapped imbalanced Fermi gas in the strongly interacting regime with small final state effects. In crossing the superfluid to normal boundary we observed a gradual crossover in the pairing mechanism by comparing majority and minority spectra. The majority spectrum shows a local double peak spectrum in the polarized superfluid region which allowed us to determine the superfluid gap  $\Delta$  and the Hartree terms  $U$ . The spectra in the normal phase are consistent with a polaron picture.

We thank W. Zwerger and M. Zwierlein for stimulating discussions and A. Sommer for critical reading of the manuscript. This work was supported by the NSF and ONR, through a MURI program, and under ARO Award W911NF-07-1-0493 with funds from the DARPA OLE program.

### Auxiliary Material: Determination of the Superfluid Gap in Atomic Fermi Gases by Quasiparticle Spectroscopy

#### Determination of the superfluid boundary

It has been shown previously [8] that at unitarity the difference column density profiles serve as an indicator for the SF-N boundary. The discontinuity of the minority density results in a pronounced "cusp" in the difference profile  $n_\uparrow(r) - n_\downarrow(r)$ , see fig. 5. In the main body of the paper the phase boundary has been determined by this peak position. Hence, "normal" refers to spatial regions beyond the peak, "superfluid" refers to spatial regions inside.

The color coding in the graphs in fig. 5 shows where the spectral overlap (definition see below) between the majority and minority pairing peaks is lost. On resonance ( $B = 690$  G) this position shows excellent agreement with the position of the cusp in the difference density profile and can therefore serve as an alternative indicator for the SF-N boundary. This coincidence breaks down away from resonance: On the BCS side ( $B = 710$  G) the spectra are less "robust" against polarization and spectral overlap is lost before the column density difference shows a peak. The reverse situation occurs on the BEC side of the resonance ( $B = 671$  G). Note that on the BEC side the minority cloud does not extend much further than the peak position in the column density difference.

#### Quantification of spectral overlap

In order to calculate the spectral overlap of a spectrum, the quasiparticle peak was fitted by a gaussian and subtracted from the majority spectrum. The overlap is then defined as one minus the difference of the integrated

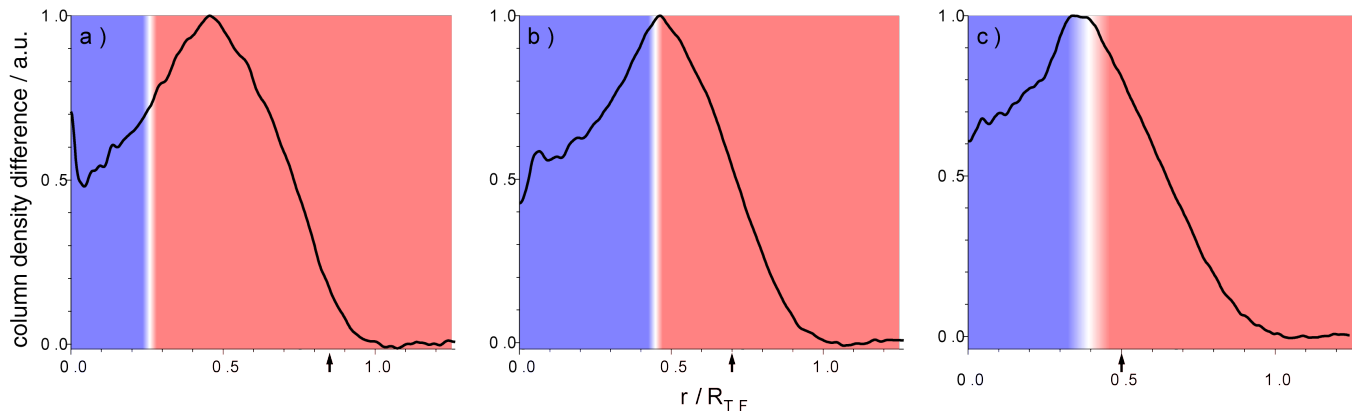


FIG. 5: (Color online) The difference column density profile  $n_{\uparrow}(r) - n_{\downarrow}(r)$  (radially averaged). a) BCS side ( $B = 710G$ ), b) Unitary limit ( $B = 690G$ ), c) BEC side ( $B = 671G$ ). Each profile shown is the average of 10 individual profiles. Blue marks the region of complete spectral overlap between majority and minority components, red marks the region where there is no complete spectral overlap. The black arrows at the bottom indicate the radial size of the minority component.

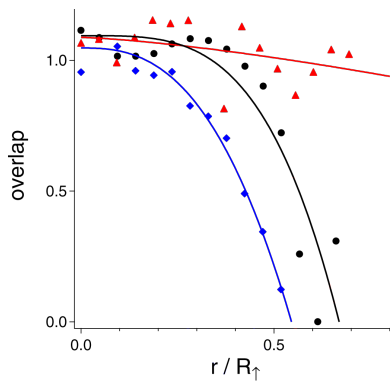


FIG. 6: (color online) Overlap of majority and minority pairing peak as a function of position in the trap for various interaction strengths. A power law was fitted to the curves as a guide to the eye. Unitary limit (black circles):  $1/k_{F\uparrow}a = 0$ , phase boundary at  $r_c/R_{\uparrow} \simeq 0.46$ ; BEC side (red triangles):  $1/k_{F\uparrow}a = 0.39(1)$ ,  $r_c/R_{\uparrow} \simeq 0.45$ ; and BCS side (blue diamonds):  $1/k_{F\uparrow}a = -0.25(1)$ ,  $r_c/R_{\uparrow} \simeq 0.35$

spectra normalized by the sum of the integrated spectra, see fig. 6. As mentioned in the main text and above, on the BEC side of the Feshbach resonance almost complete spectral overlap can be observed into the normal region. On the BCS side the reverse situation occurs.

#### Minority peak shift for high imbalance

Fig. 4 in the main body of the text shows the peak positions normalized by the local majority Fermi energy  $\epsilon_{F\uparrow}$ . Fig. 7 shows the bare peak positions as observed in the experiment.

One unexpected finding in fig. 4a in the main body of the text is the sudden increase of the minority peak po-

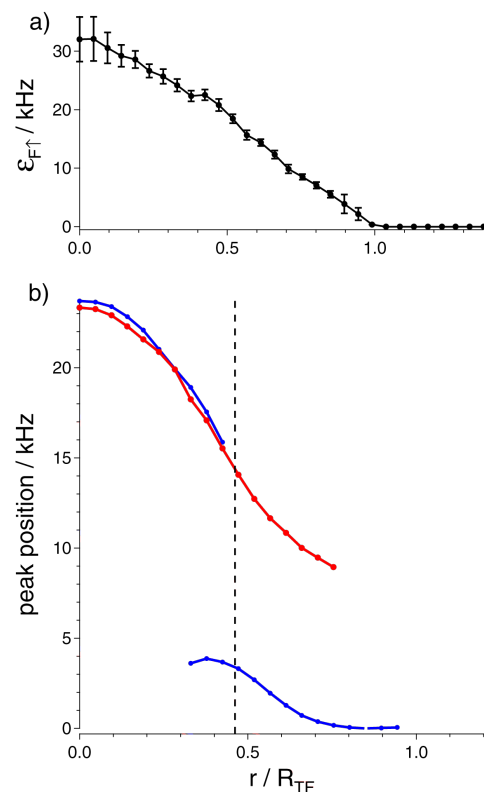


FIG. 7: (color online) a) Local majority Fermi energy in kHz, the error bars are the standard deviation of the mean value. b) Peak positions of majority and minority in kHz. Majority (Blue): Pairing peak (higher frequencies, only discernible in the SF region) and quasiparticle peak (lower frequencies). Minority (red): The peak can be traced well into the normal region.

sition for high imbalances. This behavior can be traced back to the data in fig. 7: The minority peak position

(red) shows a change in curvature as the SF-N boundary is crossed, in contrast to the majority Fermi energy. Therefore, the ratio of minority peak and majority Fermi energy shows a sudden increase towards the edges of the cloud. The value of the peak position of  $\omega_{pol} \simeq 0.9 \epsilon_{F\uparrow}$  (where final state interactions of  $E_{final} \simeq 0.05 \epsilon_{F\uparrow}$  have been taken into account) is higher than the theoretically calculated value of  $\simeq 0.6 \epsilon_{F\uparrow}$  [4].

### Quasiparticles in an equal mixture

In a previous publication [16] low temperature RF spectra did not show any signatures of quasiparticles. We have attempted to create thermally generated quasiparticles in an equal density mixture for higher temperatures  $T/T_F \geq 0.20$ . The experimental results in fig. 8 show a decrease of the gap parameter, but no local double peak structures could be resolved for any temperature.

We can estimate the temperature required to populate quasiparticles, assuming that the temperature has to be on the order of the gap and that  $\Delta(T)$  is given by the BCS relation  $\frac{\Delta(T)}{\Delta_0} = 1.74 \sqrt{1 - \frac{T}{T_c}}$  [?]. At unitarity,  $\Delta_0/T_c \simeq 3$ . One would expect to populate quasiparticles only very close to the transition temperature  $T/T_c \simeq 0.95$ , when the gap is only one third of its low-temperature value.

### The theoretical dissociation spectrum including the Hartree term $U$

Starting from a BCS-Leggett mean-field wavefunction and applying Fermi's Golden Rule, the RF spectrum can be described by (neglecting the Hartree term):

$$\Gamma(\omega) \propto \frac{\sqrt{\omega - \omega_{th}}}{\omega^2} \sqrt{1 + \frac{\omega_{th}}{\omega} + \frac{2\mu}{\omega}} \quad (1)$$

where  $\omega_{th} = \sqrt{\Delta^2 + \mu^2} - \mu$  is the dissociation threshold and  $\mu$  is the chemical potential.

The corresponding quasiparticle dispersion relation is:

$$E_k = \sqrt{\Delta^2 + (\epsilon_k - \mu)^2} \quad (2)$$

$\epsilon_k$  being the free particle dispersion  $\epsilon_k = \frac{\hbar^2 k^2}{2m}$ .

Hartree terms  $U$  modify the quasiparticle excitation spectrum [12, 30]:

$$E_k = \sqrt{\Delta^2 + (\epsilon_k - (\mu - U))^2} \quad (3)$$

resulting in an RF spectrum of

$$\Gamma(\omega') \propto \frac{\sqrt{\omega' - \omega'_{th}}}{\omega'^2} \sqrt{1 + \frac{\omega'_{th}}{\omega'} + \frac{2\mu'}{\omega'}} \quad (4)$$

where  $\omega' = \omega + U$ ,  $\omega'_{th} = \omega_{th} + U$  and  $\mu' = \mu - U$ . This demonstrates that the spectrum retains its functional form but the entire spectrum is shifted by  $U$ .

### Resolution / Experimental broadening

For comparison with the theoretical spectrum, we model the RF pulse of  $T = 200 \mu s$  length as a square pulse, in the frequency domain, resulting in a FWHM of the RF spectral power of  $\Delta\nu = 2 \cdot \frac{1}{2\pi} 1.39 \frac{2}{T} \simeq 4.4$  kHz. The theoretical spectrum consists of two parts: 1) A dissociation peak including the Hartree energy, described by eqn. 1 with  $\Delta$  and  $U$  as given in table I in the main text. 2) A quasiparticle peak modeled as a narrow (FWHM = 1 kHz) Lorentzian with a peak height adjusted so that it resembles our data. This spectrum was convolved with the Fourier transform of a square pulse  $f(\omega) \propto \frac{\sin^2 \frac{\omega T}{2}}{(\frac{\omega T}{2})^2}$ .

Fig. 9 shows that the theoretical spectrum reproduces our data quite well. The deviation in 9b) might be attributed to additional broadening mechanisms like finite quasiparticle lifetime, finite temperature and atomic diffusion during the duration of the RF pulse. The convolution causes a small shift of  $0.05 \epsilon_{F\uparrow}$  in the spectral peak position due to the asymmetry of the theoretical spectrum and has been accounted for in the determination of  $\Delta$  and  $U$ .

The value given above for the experimental resolution is confirmed by looking at the blurring of the sharp onset of pair dissociation. Equation 1 predicts that the threshold and peak position in the strongly interacting regime differ by less than 10% of the Fermi energy. Adjusting the experimental resolution to  $\sim 4$  kHz accounts for the experimentally observed difference of threshold and peak position of about  $0.3 \epsilon_{F\uparrow}$ .

- 
- [1] J. Bardeen, L. N. Cooper, and J. R. Schrieffer, Phys. Rev. **108**, 1175 (1957).
  - [2] P. A. Lee, N. Nagaosa, and X.-G. Wen, Rev. of Mod. Phys. **78**, 17 (2006).
  - [3] A. A. Abrikosov and L. Gork'ov, JETP **12**, 1243 (1961).
  - [4] F. Chevy, Phys. Rev. A **74**, 063628 (2006).
  - [5] R. Combescot, A. Recati, C. Lobo, and F. Chevy, Phys. Rev. Lett. **98**, 180402 (2007).
  - [6] N. Prokof'ev and B. Svistunov, Phys. Rev. B **77**, 020408 (2008).
  - [7] P. Massignan, G. M. Bruun, and H. T. C. Stoof (2008), preprint, arXiv:0805.3667.
  - [8] Y. Shin, C. H. Schunck, A. Schirotzek, and W. Ketterle, Nature **451**, 689 (2008).
  - [9] A. M. Clogston, Phys. Rev. Lett. **9**, 266 (1962).
  - [10] B. S. Chandrasekhar, Appl. Phys. Lett. **1**, 7 (1962).
  - [11] I. Giaever, Phys. Rev. Lett. **5**, 147 (1960).
  - [12] Y. Castin (IOS Press, Amsterdam, 2008), pp. 289–350.
  - [13] M. W. Zwierlein, A. Schirotzek, C. H. Schunck, and W. Ketterle, Science **311**, 492 (2006).
  - [14] G. B. Partridge et al., Science **311**, 503 (2006).
  - [15] Y. Shin, C. H. Schunck, A. Schirotzek, and W. Ketterle, Phys. Rev. Lett. **99**, 090403 (2007).
  - [16] C. H. Schunck, Y. Shin, A. Schirotzek, and W. Ketterle,

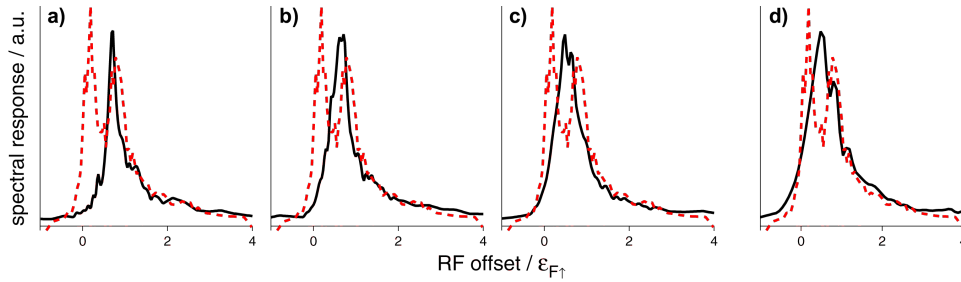


FIG. 8: (Color online) Local RF spectra of an equal spin mixture for various normalized local temperatures  $T/T_{F\uparrow}$ . a)  $T/T_{F\uparrow} \simeq 0.20$ , b)  $T/T_{F\uparrow} \simeq 0.22$ , c)  $T/T_{F\uparrow} \simeq 0.34$ , d)  $T/T_{F\uparrow} \simeq 0.55$ . No local double peak spectrum can be resolved in the RF spectrum. For comparison, the double peak spectrum of an imbalanced mixture with  $T/T_{F\uparrow} \simeq 0.06$  is added with a red dashed line.

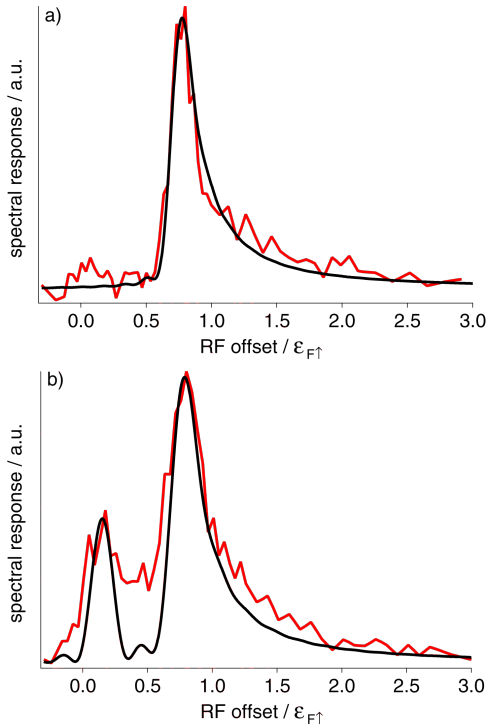


FIG. 9: (color online) Comparison of experimental (red) and theoretical (black) line shapes for spectra a) and b) of figure 1 of the main body of the paper. The theoretical curve is obtained from a BCS-Leggett mean field description including the Hartree term and a convolution with the experimental resolution of  $\simeq 4.4$  kHz. The values for  $\Delta$  and  $U$  as calculated from the peak positions lead to a reasonable agreement with the data.

- preprint, arXiv:0802.0341v2.
- [17] M. Bartenstein et al., Phys. Rev. Lett. **94**, 103201 (2004).
  - [18] W. Ketterle and M. W. Zwierlein (IOS Press, Amsterdam, 2008), pp. 95–288.
  - [19] R. Grimm (IOS Press, Amsterdam, 2008), pp. 413–462.
  - [20] D. Jin and C. Regal (IOS Press, Amsterdam, 2008), pp. 1–94.
  - [21] D. E. Sheehy and L. Radzihovsky, Ann. Phys. **322**, 1790 (2007).
  - [22] See EPAPS Document No. [XXX] for further information.
  - [23] P. Massignan, G. M. Bruun, and H. T. C. Stoof, Phys. Rev. A **77**, 031601 (2008).
  - [24] E. J. Mueller, preprint, arXiv:0711.0182v1.
  - [25] C. Chin et al., Science **305**, 1128 (2004).
  - [26] C. H. Schunck et al., Science **316**, 867 (2007).
  - [27] M. Punk and W. Zwerger, Phys. Rev. Lett. **99**, 170404 (2007).
  - [28] M. Veillette et al., preprint, arXiv:0803.2517v1.
  - [29] A. Perali, P. Pieri, and G. C. Strinati, Physical Review Letters **100**, 010402 (2008).
  - [30] A. Bulgac, J. E. Drut, P. Magierski, and G. Wlazlowski, preprint, arXiv:0801.1504v1.
  - [31] J. Carlson and S. Reddy, Phys. Rev. Lett. **95**, 060401 (2005).
  - [32] C. Lobo, A. Recati, S. Giorgini, and S. Stringari, Phys. Rev. Lett. **97**, 200403 (2006).
  - [33] S. C. R. Haussmann, W. Rantner and W. Zwerger, Phys. Rev. A **75**, 023610 (2007).
  - [34] J. Carlson and S. Reddy, Phys. Rev. Lett. **100**, 150403 (2008).
  - [35] J. C. G.E. Astrakharchik, J. Boronat and S. Giorgini, Phys. Rev. Lett. **93**, 200404 (2004).